



THE EFFECT OF NONLINEAR DAMPING ON THE UNIVERSAL ESCAPE OSCILLATOR

MIGUEL A. F. SANJUÁN

*Departamento de Ciencias Experimentales e Ingeniería,
Escuela Superior de Ciencias Experimentales y Tecnología,
Universidad Rey Juan Carlos, Tulipán s/n, 28933 Móstoles, Madrid, Spain*

Received July 1, 1998; Revised September 16, 1998

This paper analyzes the role of nonlinear dissipation on the universal escape oscillator. Nonlinear damping terms proportional to the power of the velocity are assumed and an investigation on its effects on the dynamics of the oscillator, such as the threshold of period-doubling bifurcation, fractal basin boundaries and how the basins of attraction are destroyed, is carried out. The results suggest that increasing the power of the nonlinear damping, has similar effects as of decreasing the damping coefficient for a linearly damped case, showing the very importance of the level or amount of energy dissipation.

1. Introduction

Much of the discussion in the physics and engineering literature concerning damped oscillations, focuses on systems subject to viscous damping, that is, damping proportional to the velocity, even though viscous damping occurs rarely in physical systems. Naturally, one of the benefits of its use is the introduction of a linear term in the differential equation modeling the system, which makes it easy to analyze. Other types of dissipative forces, such as Coulomb damping or aerodynamic drag exist and are present in real systems. Nevertheless, they are usually neglected, since their presence leads to nonlinear terms in the differential equation, making the system much more difficult to analyze. This is why in describing many oscillatory phenomena that occurs in nature, nonlinear oscillators with linear damping terms have been considered.

It is known also that frictional or drag forces which describe the motion of an object through a fluid or gas are rather complicated, and different phenomenological models have been proposed. One of the simplest empirical mathematical model is taken to be of the form $f(v) \propto v|v|^{p-1}$, where

v represents the velocity of the object and p , an integer, the damping exponent.

Phenomenological models describing some type of nonlinear dissipation have been used in some applied sciences such as ship dynamics [Bikdash *et al.*, 1994; Falzarano *et al.*, 1992], where a particular interest has deserved the role played by different damping mechanisms in the formulation of ship stability criteria, and vibration engineering (see e.g. [Ravindra & Mallik, 1994a, 1994b] and references therein).

Damping in certain applied systems play an important role, since it may be used to suppress large amplitude oscillations or various instabilities, and it can be also used as a control mechanism. The role of nonlinear dissipation in double-well Duffing oscillators has received some attention recently by [Ravindra & Mallik, 1994a, 1994b], where a single nonlinear damping term proportional to the power of the velocity is used and one of the conclusions is that nonlinear damping terms affect especially the onset of the period-doubling route to chaos. Sanjuán [1998] analyzed how the introduction of nonlinear damping terms of this kind affects

the structure of a chaotic attractor of a double-well Duffing oscillator and the simple pendulum, and it has been observed that the Lyapunov dimension, which provides information about how the form of the attractor is altered, decreases when the damping exponent p increases.

Numerous physical phenomena of oscillatory nature appearing in different disciplines present the ability to escape from a potential well, and are described by a universal escape nonlinear oscillator model. This nonlinear oscillator has a simple mechanical interpretation, since it describes the motion of a particle of unit mass in the single cubic potential $V(x) = x^2/2 - x^3/3$ sinusoidally driven, and is considered as a prototype for escape phenomena. When a linear dissipative force is introduced, its equation of motion is

$$\ddot{x} + \beta\dot{x} + x - x^2 = F \sin \omega t, \quad (1)$$

where β represents the damping level, F the forcing amplitude and ω the frequency of the external perturbation.

Extensive numerical and analytical studies on different aspects related to this simple nonlinear oscillator have been carried out by [Thompson *et al.*, 1987; Thompson, 1989, 1990; Thompson & Soliman, 1990; Soliman & Thompson, 1991, 1992; Stewart *et al.*, 1991; Soliman, 1994]. Analytical work related to the escape from the potential well was examined by Szemplińska-Stupnicka and Rudowski [1996] and Chacón *et al.* [1997], and a comparative analysis of the homoclinic bifurcation sets for the quasiperiodically and parametrically driven escape oscillator was done by Sanjuán [1996]. Besides that, an experimental apparatus was constructed to mimic the equation and is described in [Gottwald *et al.*, 1995].

Of special interest to the investigation reported here is the comprehensive study on the effect of damping on basin and steady-state bifurcation patterns of this oscillator, which is reported in [Soliman & Thompson, 1992].

In particular they investigated the effect of damping on the resonance response curves and how the main bifurcation boundaries, such as period-doubling bifurcation and boundary crisis, where the system escapes, are affected. (see [Alligood *et al.*, 1997] for a basic and rigorous description of boundary crises and the associated concept of transient chaos.) They have also showed how the damping level affects the erosion of the nonescaping basin.

Basically its main results are that once the parameters of the system are fixed, decreasing the damping level produces the effect of shifting backwards in parameter space the period-doubling bifurcation and the final boundary crisis leading to escape, destroying the safe basins and increasing the basin erosion patterns. As a consequence, it suggests the use of damping to suppress large scale erosion of the basin.

In the present work the effect of using nonlinear damping terms on the universal escape oscillator is considered. Even though some authors [Thompson & Soliman, 1990; Gottwald *et al.*, 1995] mention the possible interesting role played by considering nonlinear damping terms, they only contemplated linear damping terms. Nonlinear damping terms are of diverse nature and we choose here strictly dissipative nonlinear damping terms proportional to the p th power of velocity. Taking nonlinear damping terms of different damping exponents, we carry out a comprehensive study on how these affect the dynamics of the oscillator, the main bifurcations and the basin of attraction patterns when different periodic attractors may coexist prior to escape from the potential well. The obtained numerical results show evidence that the period-doubling bifurcations and boundary crises leading to escape shift backwards in parameter space. An analytical study using Melnikov theory predicts rather well a shift of this kind in the computation and numerical observation of the appearance of the fractal basin boundaries [Moon & Li, 1985; McDonald *et al.*, 1985]. On the other hand different numerical experiments show that increasing the damping exponent strongly influences the erosion pattern of the basin. All these phenomena suggest that fixing parameters of the system and varying only the damping exponent p , taking integer values, has similar effects as decreasing the damping level for the linear damping case.

2. The Nonlinearly Damped Universal Escape Oscillator

Soliman and Thompson [1992] have studied with considerable detail the effects of the damping level on the resonance response of the steady-state solutions and in the basin bifurcation patterns of the escape oscillator. In particular they analyzed the effect of using different damping levels and how this contributes to the erosion of the safe areas in phase

space, and they also provide a comprehensive global picture of the main bifurcation boundaries.

Here we consider the same equation used by them, but with a nonlinear damping term instead. The equation of motion for the sinusoidally driven escape oscillator including nonlinear damping terms as a power series on the velocity reads

$$\ddot{x} + \sum_{p=1}^n \beta \dot{x} |\dot{x}|^{p-1} + x - x^2 = F \sin \omega t, \quad (2)$$

where β is the damping level, p is the damping exponent, and F and ω the forcing amplitude and the frequency of the external perturbation, respectively. In particular the model equation we consider is

$$\ddot{x} + \beta \dot{x} |\dot{x}|^{p-1} + x - x^2 = F \sin \omega t, \quad (3)$$

where for simplicity only a single damping term proportional to the p th power of the velocity is taken. A similar nonlinear damping term was used by Bikdash *et al.* [1994], Ravindra and Mallik [1994a, 1994b] and Sanjuán [1998].

The dynamics of the escape oscillator has been simulated using a fixed-step-size fourth-order Runge–Kutta numerical integration and the associated two-dimensional Poincaré map.

We want to analyze the main features of the steady-state solutions of the system for different values of p . As in [Soliman & Thompson, 1992], for most of our numerical computations we use a fixed frequency $\omega = 0.85$ and a damping level $\beta = 0.1$ and when we modify the damping exponent p , we observe strong erosions in the basins as the damping parameter p increases. The effect is similar to keeping fixed all parameters and decreasing the forcing term. For $p = 1$ and for the initial condition $(0.175, -0.55)$, which is close to a fixed point attractor, a nice Feigenbaum period-doubling cascade in the forcing parameter range $0.1 \leq F \leq 0.109$ is found (this corresponds to the result shown in [Thompson *et al.*, 1987; Thompson, 1989]). Soliman and Thompson, [1992] indicate that reducing the damping level implies that the period-doubling-escape scenario, which is typically observed, takes place at lower forcing amplitudes. In particular they study the influence of modifying the forcing and damping level. When a quadratic nonlinear damping is used, that is $p = 2$, and for the same initial condition as before, a chaotic cascade in the parameter range $0.087 \leq F \leq 0.096$ appears, and this is shown in Fig. 1. One of the effects of using the quadratic nonlinear damping is precisely the

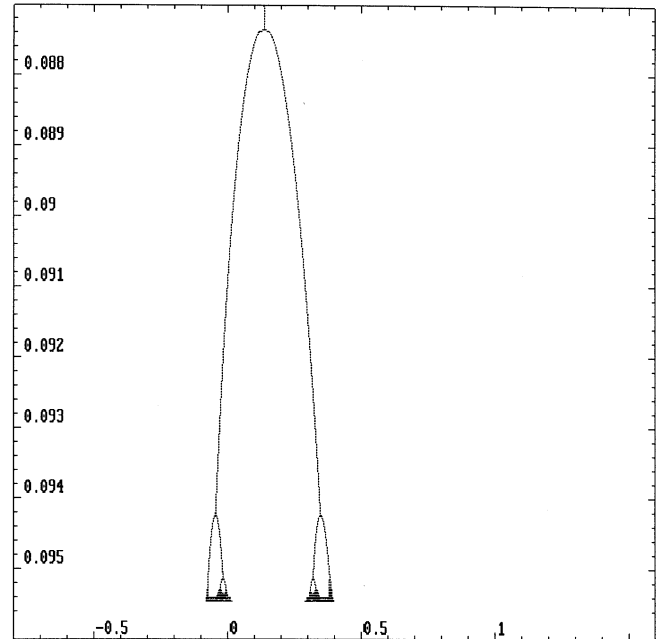


Fig. 1. Plot of the period-doubling bifurcation diagram of the nonlinear escape oscillator with equation $\ddot{x} + 0.1\dot{x}|\dot{x}| + x - x^2 = F \sin 0.85t$ for the initial condition $(0.175, -0.55)$. The variation of the forcing amplitude is $0.086 < F < 0.096$.

lowering of the critical forcing for which the homoclinic bifurcation and the escape boundary take place. In particular for $F = 0.0954$, the result is a beautiful two-piece chaotic attractor with a Lyapunov dimension $D_L = 1.22$. This chaotic attractor is shown in Fig. 2, where the two pieces are clearly seen in the blowup in the inset (the rectangle $(-0.2, 0.5) \times (-0.6, -0.4)$).

When $p = 3$, that is a cubic nonlinear damping, chaotic solutions are found as well in the parameter region $0.083 \leq F \leq 0.093$. Consequently it appears to be a shift backwards in the period-doubling bifurcation threshold and escape as the damping exponent p is increased. If our numerical experiments are compared to the results shown for the linear damping case ($p = 1$) by [Soliman & Thompson, 1992]) we may conclude that increasing the damping exponent p has similar effects as decreasing the damping level β . There is a rather intuitive argument to justify this behavior. Think for simplicity in a particle moving with certain energy inside the potential well. Using topological arguments concerning the phase space of the escape oscillator, the velocity $\dot{x}(t)$ is bounded and $|\dot{x}(t)| < 1$ for all times, for any motion inside the potential well. This being so, it implies that $|\dot{x}(t)|^p < |\dot{x}(t)| < 1$, for $p > 1$. So this explains intuitively the observations of the

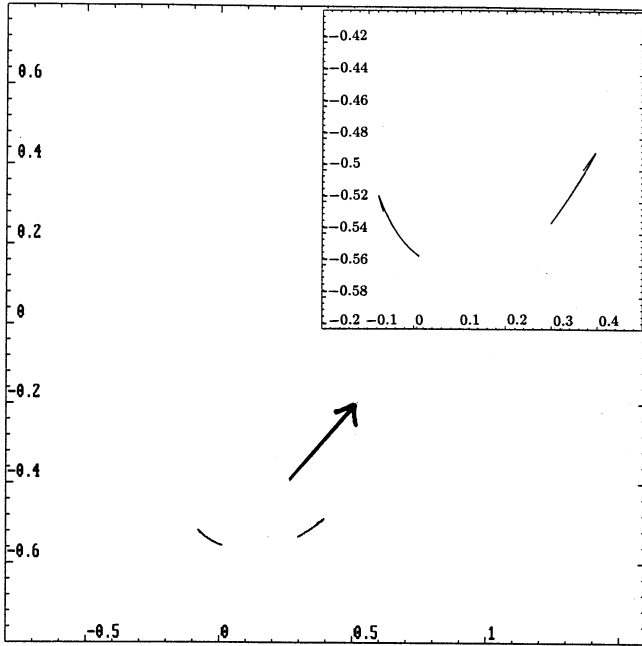


Fig. 2. Plot of the two-piece chaotic attractor of the nonlinear escape oscillator with equation $\ddot{x} + 0.1\dot{x}|\dot{x}| + x - x^2 = 0.0954 \sin 0.85t$ for the initial condition $(0.175, -0.55)$. Its Lyapunov dimension is 1.22. In the inset of size $(-0.2, 0.5) \times (-0.4, -0.6)$ appears a blow up of the chaotic attractor.

numerical experiments carried out for different values of the damping exponent, since using a parameter $p > 1$ implies a reduction of the damping term which numerically is equivalent to using the linear damping term with a lower damping level.

3. Melnikov Analysis for the Nonlinear Damping Case

The numerical results obtained in the previous section suggest that when a nonlinear damping term is used instead of a linear damping term the global pattern of bifurcations is affected. The Melnikov analysis provides an analytical estimate of the parameters for which homoclinic bifurcations occur, and as was proved by Moon and Li [1985], the critical parameters derived from this analysis signal the appearance of fractal basin boundaries between co-existing attractors.

Our aim here is to apply the Melnikov method to the nonlinearly damped and sinusoidally forced escape oscillator

$$\ddot{x} + \beta\dot{x}|\dot{x}|^{p-1} + x - x^2 = F \sin \omega t, \quad (4)$$

where $p \geq 1$ is the damping exponent. In the absence of forcing and damping this system is com-

pletely integrable and it has a separatrix orbit (homoclinic orbit) in phase space, which divides it in two regions, one of bounded motions and one of unbounded motions. Only the points inside the separatrix correspond to bounded motions and the inclusion of an external perturbation leads to the possibility of escape to infinity. The equations of motion of the separatrix orbit of the unperturbed system are

$$x_{sx}(t) = \frac{3}{2} \tanh^2 \frac{t}{2} - \frac{1}{2} \quad (5)$$

$$y_{sx}(t) = \frac{3}{2} \frac{\sinh \frac{t}{2}}{\cosh^3 \frac{t}{2}}. \quad (6)$$

When the damping and the forcing are taken into account as a small perturbation to the unperturbed system, there is an associated Melnikov function which is given by

$$M(t_0, \omega, p) = \int_{-\infty}^{+\infty} y_{sx}(t)F \sin \omega(t + t_0)dt - \int_{-\infty}^{+\infty} \alpha_p y_{sx}^{p+1}(t)dt, \quad (7)$$

where $y_{sx}(t)$ corresponds to the separatrix. Thus the Melnikov function can be written as

$$M(t_0, \omega, p) = \frac{3}{2} F \cos \omega t_0 \int_{-\infty}^{+\infty} \text{sech}^2 \frac{t}{2} \tanh \frac{t}{2} \sin \omega t dt - \beta \left(\frac{3}{2}\right)^{p+1} \int_{-\infty}^{+\infty} \left(\frac{\sinh \frac{t}{2}}{\cosh^3 \frac{t}{2}}\right)^{p+1} dt. \quad (8)$$

The evaluation of the integrals gives the result

$$M(t_0, \omega, p) = \frac{6\pi\omega^2 F \cos \omega t_0}{\sinh[\pi\omega]} - 2\beta \left(\frac{3}{2}\right)^{p+1} B\left(\frac{p+2}{2}, p+1\right), \quad (9)$$

where $B(m, n)$ is the Euler Beta function, which can be easily evaluated in terms of the Euler Gamma function [Abramowitz & Stegun, 1970].

The critical forcing parameter F_{cp} for which homoclinic tangles intersect, that for a certain frequency ω depends on the damping exponent p and the damping coefficient β , may be written as

$$F_{cp} = \beta \frac{\sinh[\pi\omega]}{3\pi\omega^2} \left(\frac{3}{2}\right)^{p+1} B\left(\frac{p+2}{2}, \frac{p+1}{2}\right). \tag{11}$$

When more nonlinear damping terms are considered, then the Melnikov function takes the form of

$$M(t_0, \omega, p) = \frac{6\pi\omega^2 F \cos \omega t_0}{\sinh[\pi\omega]} - \sum_{p=1}^n 2\beta \left(\frac{3}{2}\right)^{p+1} B\left(\frac{p+2}{2}, p+1\right), \tag{12}$$

and consequently the critical parameter of the external perturbation is given by

$$F_{cp} = \sinh[\pi\omega] \sum_{p=1}^n \frac{\beta}{3\pi\omega^2} \left(\frac{3}{2}\right)^{p+1} B\left(\frac{p+2}{2}, \frac{p+1}{2}\right). \tag{13}$$

This expression gives an idea of the effect of the nonlinear damping terms on the threshold of homoclinic chaos and the associated appearance of fractal basin boundaries.

The Melnikov ratio $R(\omega, p)$ represents the ratio of the forcing to the damping level (F_{cp}/β), which obviously depends on the frequency ω and

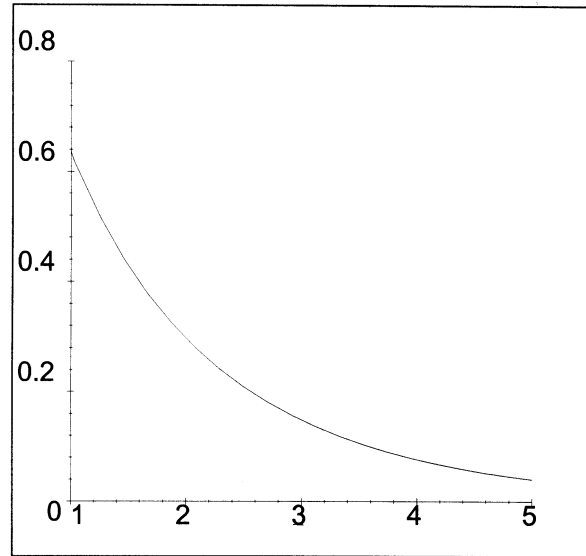
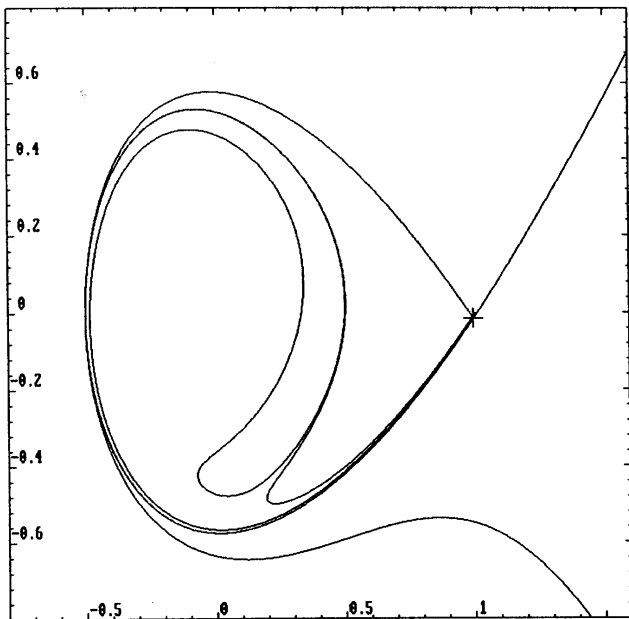
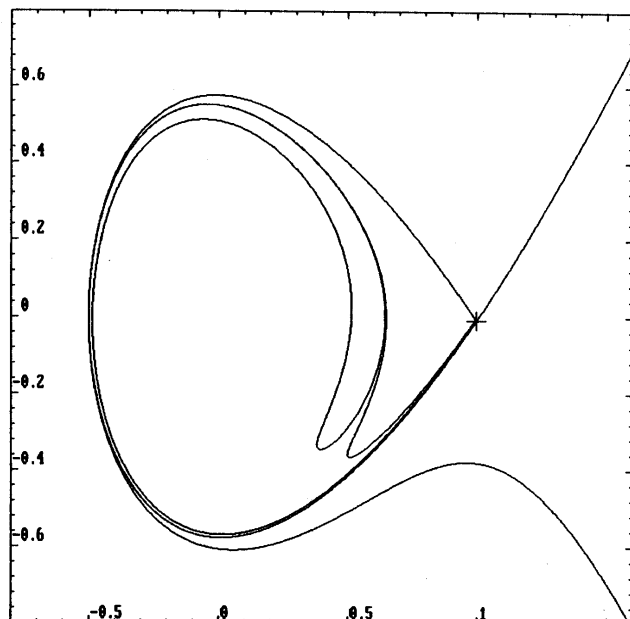


Fig. 3. The Melnikov ratio $R(\omega, p) = F_{cp}/\beta$ versus the damping exponent p is plotted. Here is the evidence for higher values of the damping exponent, the critical forcing necessary for the fractalization of the boundaries decreases.



(a)



(b)

Fig. 4. The figure shows the homoclinic tangency for different nonlinear damping terms, as calculated with the help of Melnikov theory. (a) For a quadratic nonlinear damping term, $p = 2$, $\beta = 0.1$, and $F = 0.0297$. (b) For a cubic nonlinear damping term, $p = 3$, $\beta = 0.1$, and $F = 0.0148$.

the damping exponent p . According to Eq. (11) it takes the expression

$$R(\omega, p) = \frac{\sinh[\pi\omega]}{3\pi\omega^2} \left(\frac{3}{2}\right)^{p+1} B\left(\frac{p+2}{2}, \frac{p+1}{2}\right). \quad (14)$$

Figure 3 depicts the variation of the Melnikov ratio $R(\omega, p)$ with the damping exponent p , which shows a decaying dependence on p . Hence when a nonlinear damping term is used instead of a linear damping term, with a fixed damping level β , then the critical forcing for fractal basin boundaries to occur decreases. In the case of linear damping, $p = 1$, the Melnikov ratio is given by $R(\omega, 1) = \sinh[\pi\omega]/5\pi\omega^2$ and the critical forcing, when $\omega = 0.85$, is $F = 0.633 \times \beta$, which is the expression obtained by Thompson *et al.* [1987] and Thompson [1989]. The critical forcing terms for the quadratic and cubic nonlinear damping, with damping level $\beta = 0.1$, have been explicitly calculated. Its values are $F = 0.0297$ for the quadratic case and $F = 0.0148$ for the cubic case. As was proved by Moon and Li [1985], this critical forcing gives the threshold for the fractal basin boundaries. Moreover for these critical values the invariant manifolds associated to the fixed point of saddle type of the Poincaré map associated to the escape oscillator, intersect themselves tangentially. Figure 4(a) shows the tangency of the unstable (the inset) and stable (the outset) manifolds associated to the saddle fixed point situated at $(0.999, -0.015)$, for $F = 0.0297$ and $\omega = 0.85$, with quadratic nonlinear damping. The homoclinic tangency for the invariant manifolds associated to the saddle fixed point at $(0.999, -0.007)$ for $F = 0.0148$ and $\omega = 0.85$ is shown in Fig. 4(b), when a cubic nonlinear damping is considered. The inset is the unstable manifold and the outset is the stable manifold.

4. Basins of Attraction

A basin of attraction is defined as the set of points taken as initial conditions, that are attracted to a fixed point or an invariant set (see e.g. [Alligood *et al.*, 1997] or [Nusse & Yorke, 1996b]). As it was mentioned previously, the escape oscillator may be seen as a mechanical oscillator where a particle of unit mass moves inside an asymmetrical potential well, with the possibility of escape. This means that besides the possible attractors that may coexist in the interior of the well, the infinity may be

taken as an attractor as well. The basin of attraction in this case signals the points in phase space that are attracted to a safe oscillation within the potential well, and the set of points that escape outside the potential well to the infinity. A study of these basins of attraction for the escape oscillator has been done extensively and with considerable detail by Michael Thompson and collaborators in a series of papers [Thompson *et al.*, 1987; Thompson, 1989, 1990; Thompson & Soliman, 1990; Soliman & Thompson, 1991; Stewart *et al.*, 1991; Soliman & Thompson, 1992; Soliman, 1994]. Attention is focused here, specially to the paper by Soliman and Thompson [1992], where the effect of the damping level is analyzed. What we want to study here is the effect of using nonlinear damping terms on the equation of the escape oscillator and how the basins of attraction are affected as the damping exponent p is increased. We follow two strategies. The first one consists in fixing the forcing amplitude $F = 0.05$ and for three different sets of damping levels at $\beta = 0.1$, $\beta = 0.15$ and $\beta = 0.2$ for different damping exponents, that is, linear damping, quadratic damping and cubic damping, to compute the basins of attraction. To numerically generate the basins of attraction, we select a grid of 300×300 points in the region of phase space determined by the rectangle of points $(-0.8, 1.4) \times (-0.8, 0.8)$, which are taken as initial conditions. Depending on the attractor an initial point goes to, it is assigned a different color. Those initial points which go to any attractor located in the interior of the well are assigned the color white. The color black is assigned to any initial point which escapes the potential well. These computations are shown in Fig. 5. The first column shows the basins of attraction for a fixed value of the damping level, $\beta = 0.1$, the second column corresponds to $\beta = 0.15$ and the third column to $\beta = 0.2$. On the other hand, the first row corresponds to damping exponent $p = 1$, that is, linear damping, the second row to $p = 2$, quadratic nonlinear damping, and the third row to $p = 3$, cubic nonlinear damping. Observing these basins of attraction in Fig. 5 it is inferred that for a fixed damping level, the increase of the damping exponent, has a clear effect on the destruction of the safe areas inside the well and the erosion of the basins increases notably. If we compare these results to the corresponding results for linear damping for which only the damping level is varied, the conclusion is that they are equivalent to a decrease of the damping level.

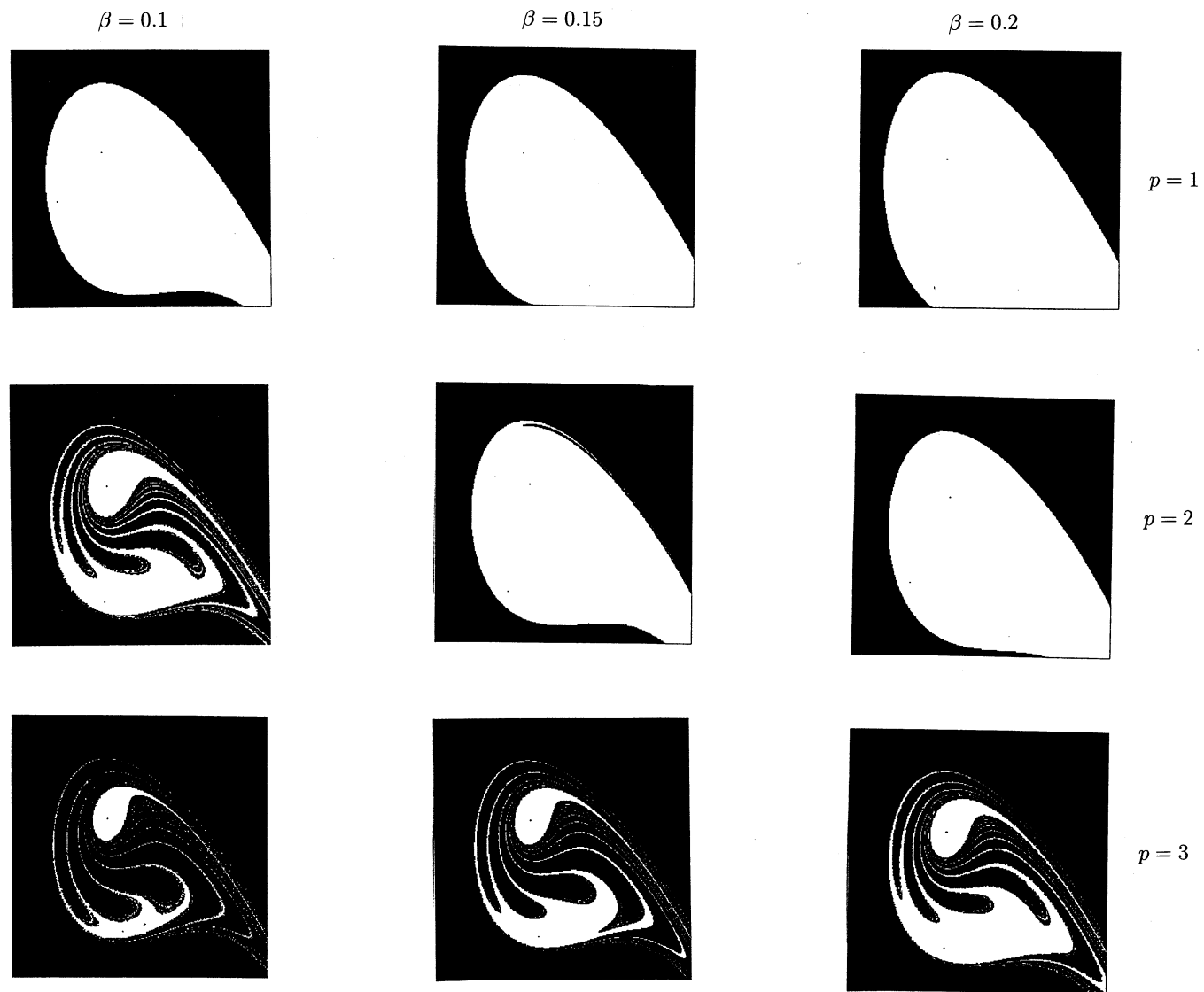


Fig. 5. The figure shows the basin erosion pattern of the escape oscillator $\ddot{x} + \beta\dot{x}|\dot{x}|^{p-1} + x - x^2 = 0.05 \sin 0.85t$. The first column corresponds to a damping level $\beta = 0.1$, the second to $\beta = 0.15$, and the third one to $\beta = 0.2$. Different rows represent different damping exponents. The first row corresponds to $p = 1$, the second row to $p = 2$ and the third row to $p = 3$.

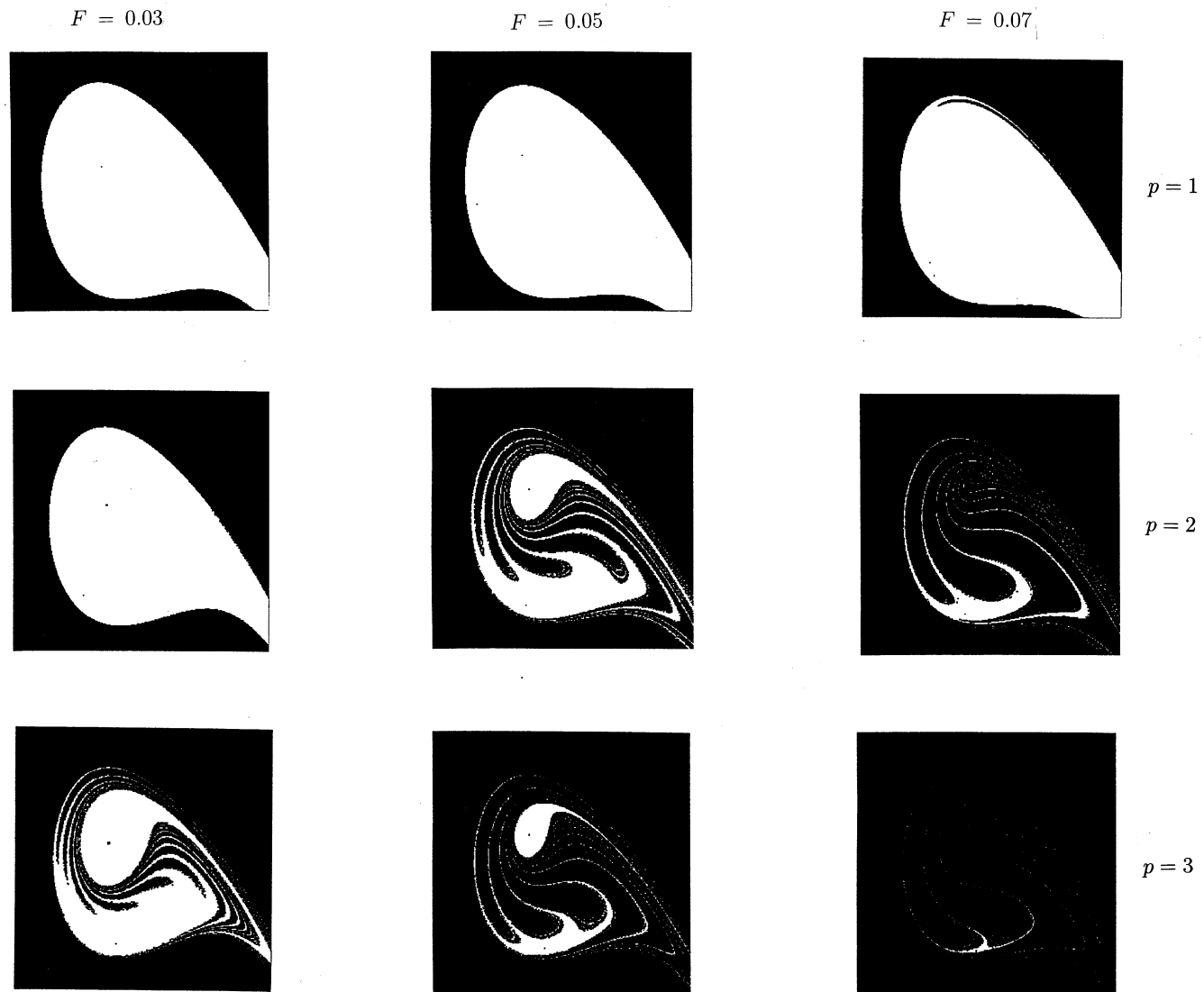


Fig. 6. Basin erosion pattern of the escape oscillator $\ddot{x} + 0.1\dot{x}|\dot{x}|^{p-1} + x - x^2 = F \sin 0.85t$. The first column corresponds to a forcing amplitude $F = 0.03$, the second to $F = 0.05$, and the third one to $F = 0.07$. Concerning rows, the first row corresponds to $p = 1$, the second row to $p = 2$ and the third row to $p = 3$.

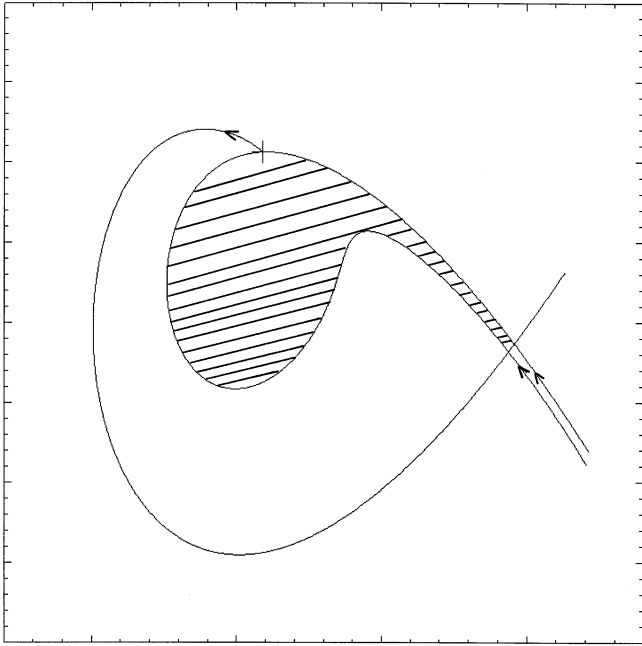


Fig. 7. Basin cell, crosshatched, of the escape oscillator with equation $\ddot{x} + 0.1\dot{x}|\dot{x}|^2 + x - x^2 = 0.03 \sin 0.85t$ generated by a period 1 orbit situated at $(0.092, 0.425)$.

The second strategy is fixing the damping level at $\beta = 0.1$ and considering different values of forcing amplitudes such as $F = 0.03$, $F = 0.05$ and $F = 0.07$ for the linear, quadratic and cubic dampings. The first column in Fig. 6 shows the basins of attraction for $F = 0.03$, the second column corresponds to $F = 0.05$ and the third column to $F = 0.07$. The rows correspond to linear, quadratic and cubic damping, respectively.

The basins in this figure show that indeed the damping exponent has a strong effect on the erosion of the basin, but the strongest effect is manifested by the increase of the forcing as it happens as well in the linear damping case. Similar heuristic arguments as the ones given in the previous sections explain this behavior.

In some of these basins shown in Figs. 5 and 6 two attractors coexist in the absence of any kind of fractalization of the boundaries. Something interesting to mention concerning most basins shown here is the presence of very clear basin cells [Nusse & Yorke, 1995, 1996a, 1996b]. The notion of a trapping region clarifies this idea. A trapping region is a region in phase space from which points cannot escape. Once the trajectory enters the region it cannot leave it and also there must be at least one attractor located there. A cell is a region in phase space whose boundary consists of the pieces

of stable and unstable curves of some periodic trajectories. When a cell is a trapping region then is a basin cell. One of these basin cells is shown crosshatched in Fig. 7, and corresponds to $p = 3$, $\beta = 0.1$ and $F = 0.03$. A period 1 orbit which generates the basin cell, which is situated at the coordinates $(0.092, 0.425)$, and the boundaries are its associated stable and unstable manifolds.

5. Conclusions

Even though attention has been paid to the study of the effect of the damping level on the dynamics of the universal escape oscillator, this has not been extended to the case of nonlinear dissipation in spite of its natural extension to some phenomenological models. The study of its effect on this nonlinear oscillator is carried out in this paper. In particular we have analyzed by numerical methods and also by using the analytical method provided by the Melnikov theory how the introduction of nonlinear damping terms affects the threshold of the period-doubling bifurcation route to chaos, the boundary crises leading to final escape to infinity and the threshold parameter for the appearance of the fractal basin boundaries. As a result, a good agreement between the analytical estimates and the numerical observations is observed. Moreover the effect of using different nonlinear damping terms on the erosion of the nonescaping basin has been studied. By fixing all the parameters of the system and varying only the damping exponent, the observation is that the increase of the damping exponent provokes a rapid erosion of the basin of attraction. When the damping level is increased a safe region increases, but it is rapidly eroded as the damping exponent also increases. Decreasing the forcing level for the linear damping case helps in the suppression of the erosion basin, but if at the same time the damping exponent is increased the situation is similar as if the forcing were increased. When the forcing is increased the erosion of the basin is bigger, and becomes even bigger if at the same time the damping exponent is increased. In the case of the linear damping and a fixed forcing, the erosion of the basin increases while the damping level is decreased, and for a fixed value of the damping level the erosion is bigger when the forcing is increased. All this suggest that the increase of the damping exponent has similar effects as of decreasing the damping level for a linearly damped model. These results are

clearly consistent with those found in [Soliman & Thompson, 1992] and show the very importance of the level or amount of energy dissipation on the dynamics of the nonlinear oscillator.

Acknowledgments

The figures were computed with the software DYNAMICS [Nusse & Yorke, 1998]. This work was supported by the Ministry of Education and Culture, Spain, project DGES PB96-0123.

References

- Abramowicz, A. & Stegun, I. [1970] *Handbook of Mathematical Functions* (Dover, NY).
- Alligood, K. T., Sauer, T. D. & Yorke, J. A. [1997] *Chaos: An Introduction to Dynamical Systems* (Springer, NY), pp. 203–207.
- Bikdash, M., Balachandran, B. & Nayfeh, A. [1994] “Melnikov analysis for a ship with a general roll-damping model,” *Nonlin. Dyn.* **6**, 101–124.
- Chacón, R., Balibrea, F. & López, M. A. [1997] “Role of parametric resonance in the inhibition of chaotic escape from a potential well,” *Phys. Lett.* **A235**, 153–158.
- Falzarano, J. M., Shaw, S. W. & Troesch, A. W. [1992], “Application of global methods for analyzing dynamical systems to ship rolling motion and capsizing,” *Int. J. Bifurcation and Chaos* **2**, 101–115.
- Gottwald, J. A., Virgin, L. N. & Dowell, E. H. [1995] “Routes to escape from an energy well,” *J. Sound Vib.* **187**, 133–144.
- McDonald, S. W., Grebogi, C., Ott, E. & Yorke, J. A. [1985] “Fractal basin boundaries,” *Physica* **D17**, 125–153.
- Moon, F. C. & Li, G.-X. [1985] “Fractal basin boundaries and homoclinic orbits for periodic motions in a two-well potential,” *Phys. Rev. Lett.* **55**, 1439–1442.
- Nusse, H. E., Ott, E. & Yorke, J. A. [1995] “Saddle-node bifurcations on fractal basin boundaries,” *Phys. Rev. Lett.* **75**, 2482–2485.
- Nusse, H. E. & Yorke, J. A. [1996a] “Wada basin boundaries and basin cells,” *Physica* **D90**, 242–261.
- Nusse, H. E. & Yorke, J. A. [1996b] “Basins of attraction,” *Science* **271**, 1376–1380.
- Nusse, H. E. & Yorke, J. A. [1998] *Dynamics: Numerical Explorations*, 2nd edition (Springer, NY).
- Ravindra, B. & Mallik, A. K. [1994a] “Stability analysis of a non-linearly damped Duffing oscillator,” *J. Sound Vib.* **171**, 708–716.
- Ravindra, B. & Mallik, A. K. [1994b] “Role of nonlinear dissipation in soft Duffing oscillators,” *Phys. Rev.* **E49**, 4950–4954.
- Sanjuán, M. A. F. [1996] “Homoclinic bifurcation sets of driven nonlinear oscillators,” *Int. J. Th. Phys.* **35**, 1745–1752.
- Sanjuán, M. A. F. [1998] “Lyapunov dimension and nonlinear dissipation,” *Phys. Rev. E*, submitted.
- Soliman, M. S. & Thompson, J. M. T. [1991] “Basin organization prior to a tangled saddle-node bifurcation,” *Int. J. Bifurcation and Chaos* **1**, 107–119.
- Soliman, M. S. & Thompson, J. M. T. [1992] “The effect of damping on the steady state and basin bifurcation patterns of a nonlinear mechanical oscillator,” *Int. J. Bifurcation and Chaos* **2**, 81–91.
- Soliman, M. S. [1994] “Predicting regimes of indeterminate jumps to resonance by assessing fractal boundaries in control space,” *Int. J. Bifurcation and Chaos* **4**, 1645–1653.
- Stewart, H. B., Thompson, J. M. T., Lansbury, A. N. & Ueda, Y. [1991] “Generic patterns of bifurcations governing the escape from a potential well,” *Int. J. Bifurcation and Chaos* **1**, 265–267.
- Szemplińska-Stupnicka & Rudowski, J. [1996] “On minimum safe impulsive velocity in the driven escape oscillator,” *Int. J. Nonlin. Mech.* **31**, 255–266.
- Thompson, J. M. T., Bishop, S. R. & Leung L. M. [1987] “Fractal basins and chaotic bifurcations prior to escape from a potential well,” *Phys. Lett.* **A121**, 116–120.
- Thompson, J. M. T. [1989] “Chaotic phenomena triggering the escape from a potential well,” *Proc. R. Soc. London* **A421**, 195–225.
- Thompson, J. M. T. [1990] “Fractal control boundaries of driven oscillators and their relevance to safe engineering design,” *Proc. R. Soc. London* **A428**, 1–13.